

LA-UR-81-3065

MASTER

TITLE: NUMERICAL MODELING OF INSENSITIVE HIGH-EXPLOSIVES INITIATION

AUTHOR(S): Allen L. Bowman and Charles L. Mader

SUBMITTED TO: Martin F. Zimmerman, Project Officer
DIA-AF-71-FG-704 Physics of Explosives Technical Meeting

University of California

By acceptance of this article for publication, you warrant that the U.S. Government retains a certain non-exclusive, irrevocable, and exclusive authority to publish or reproduce the published form of this article for up to allow others to file a copy for archival purposes.

The Los Alamos Scientific Laboratory certifies that the published herein identify this article as work performed for the direct interest of the U.S. Department of Energy.



LOS ALAMOS SCIENTIFIC LABORATORY

Post Office Box 1663 Los Alamos, New Mexico 87545

An Affirmative Action - Equal Opportunity Employer



NUMERICAL MODELING OF
INSENSITIVE HIGH-EXPLOSIVES INITIATION

Allen L. Bowman and Charles L. Mader
Los Alamos National Laboratory

ABSTRACT

The initiation of propagating, diverging detonation is usually accomplished by small conventional initiators. As the explosive to be initiated becomes more shock insensitive, the initiators must have larger diameters to be effective. Very shock-insensitive explosives have required initiators larger than 2.5 cm. We have numerically examined the process of initiation of propagating detonation as a function of the shock sensitivity of the explosive using the two-dimensional Lagrangian reactive hydrodynamic code 2DL and the Forest Fire rate to describe the shock initiation process of heterogeneous explosives. The initiation of propagating detonation in shock-insensitive explosives containing triamino trinitrobenzene results in large regions of partially decomposed explosive even when initiated by large initiators. The process has been observed experimentally and reproduced numerically.

1. INTRODUCTION

The initiation of propagating, diverging detonation is usually accomplished by small conventional initiators; however, as the explosive to be initiated becomes more shock insensitive, the initiators must have larger diameters (>2.5 cm) to be effective.

Travis¹ has used the I²C camera to examine the nature of the diverging detonation waves formed in PBX-9404 (94/3/3 HMX/nitrocellulose/Tris- β -chloroethyl phosphate), X0290 or PBX-9502 (95/5 TATB/Kel-F at 1.894 g/cm³), and X0219 (90/10 TATB/Kel F at 1.914 g/cm³) by hemispherical initiators. The geometries of the initiators were (1) a 6.35-mm-radius hemisphere of PBX-9407 (94/6 RDX/Exon at 1.61 g/cm³) surrounded by a 6.35-mm-thick hemisphere of PBX-9404, (2) a 6.35-mm-radius hemisphere of 1.7-g/cm³ TATB surrounded by a 19.05-mm-thick hemisphere of 1.8-g/cm³ TATB, or (3) a 16-mm-radius hemisphere of X0351 (15/5/80 HMX/Kel-F/TATB at 1.89 g/cm³).

We have numerically examined systems with similar geometries by use of the hydrodynamic code 2DL² and the Forest Fire rate³ to describe the shock initiation process.

II. NUMERICAL MODELING

The two-dimensional reactive Lagrangian hydrodynamic code 2DL² was used to describe the reactive fluid dynamics. The Forest Fire³ description of heterogeneous shock initiation was used to describe the explosive burn. The HOM equation of state and Forest Fire rate constants for PBX-9502, PBX-9404, and X0219 were identical to those described in Ref. 4. The Pop plots are shown in Fig. 1 and the Forest Fire rates in Fig. 2. The calculations were done in cylindrical geometry with Lucite confinement rather than the air confinement present in the experimental study. The Lucite confinement prevents the mesh distortion that can be fatal to Lagrangian calculations.

The central 6.35-mm region of the detonator is initially exploded, which initiates the remaining explosive in the detonator using a C-J volume burn. For any given mesh size and time step, the viscosity must be adjusted to give a peak pressure at the detonation front near the effective C-J pressure. The parameters used are as follows.

Calculation		Mesh Size (cm)	Time Step (μ s)	Viscosity Coefficient
Initiator	Acceptor			
PBX-9407/PBX-9404	PBX-9404	0.05	0.02	4.0
PBX-9407/PBX-9404	PBX-9502	0.05	0.02	5.0
PBX-9407/PBX-9404	X0219	0.05	0.02	4.2
1.7 TATB/1.8 TATB	PBX-9502	0.1	0.02	5.0
X0351	PBX-9502	0.1	0.02	5.0

The pressure and mass fraction contours are shown for a PBX-9404 hemisphere initiating PBX-9404 in Fig. 3, PBX-9502 (X0290) in Fig. 4, and X0219 in Fig. 5. The experimental¹ and calculated position of the leading wave as a function of distance from the origin is shown in Fig. 6.

The burn can become unstable when it turns a corner. The instability is apparently numerical because it can be eliminated by using an average of nearby cell pressures for the Forest Fire burn rather than the individual cell pressure.

The pressure and mass fraction contours are shown in Fig. 7 for the 1.8-g/cm³ TATB hemisphere initiating PBX-9502. Very little undecomposed explosive was observed experimentally, in agreement with the calculated results. The contours are shown in Fig. 8 for an X0351 hemisphere initiating PBX-9502. The experimental and calculated regions of partially decomposed PBX-9502 are shown in Fig. 9.

III. CONCLUSIONS

The initiation of propagating detonation in sensitive (PBX-9404) and insensitive (PBX-9502 and X0219) explosives by hemispherical initiators can be described numerically using the two-dimensional Lagrangian code 2DL and the Forest Fire rate. Large regions of partially decomposed explosive occur even when insensitive explosives are initiated by large initiators.

REFERENCES

1. James R. Travis. Los Alamos National Laboratory, personal communication.
2. J. N. Johnson, C. L. Mader, and M. S. Shaw, "2DL: A Lagrangian Two-Dimensional Finite-Difference Code for Reactive Media," Los Alamos National Laboratory report LA-8922-M (August 1981).
3. C. A. Forest, "Burning and Detonation," Los Alamos Scientific Laboratory report LA-7245 (July 1978).
4. Charles L. Mader, Numerical Modeling of Detonations (University of California Press, Berkeley, 1979).

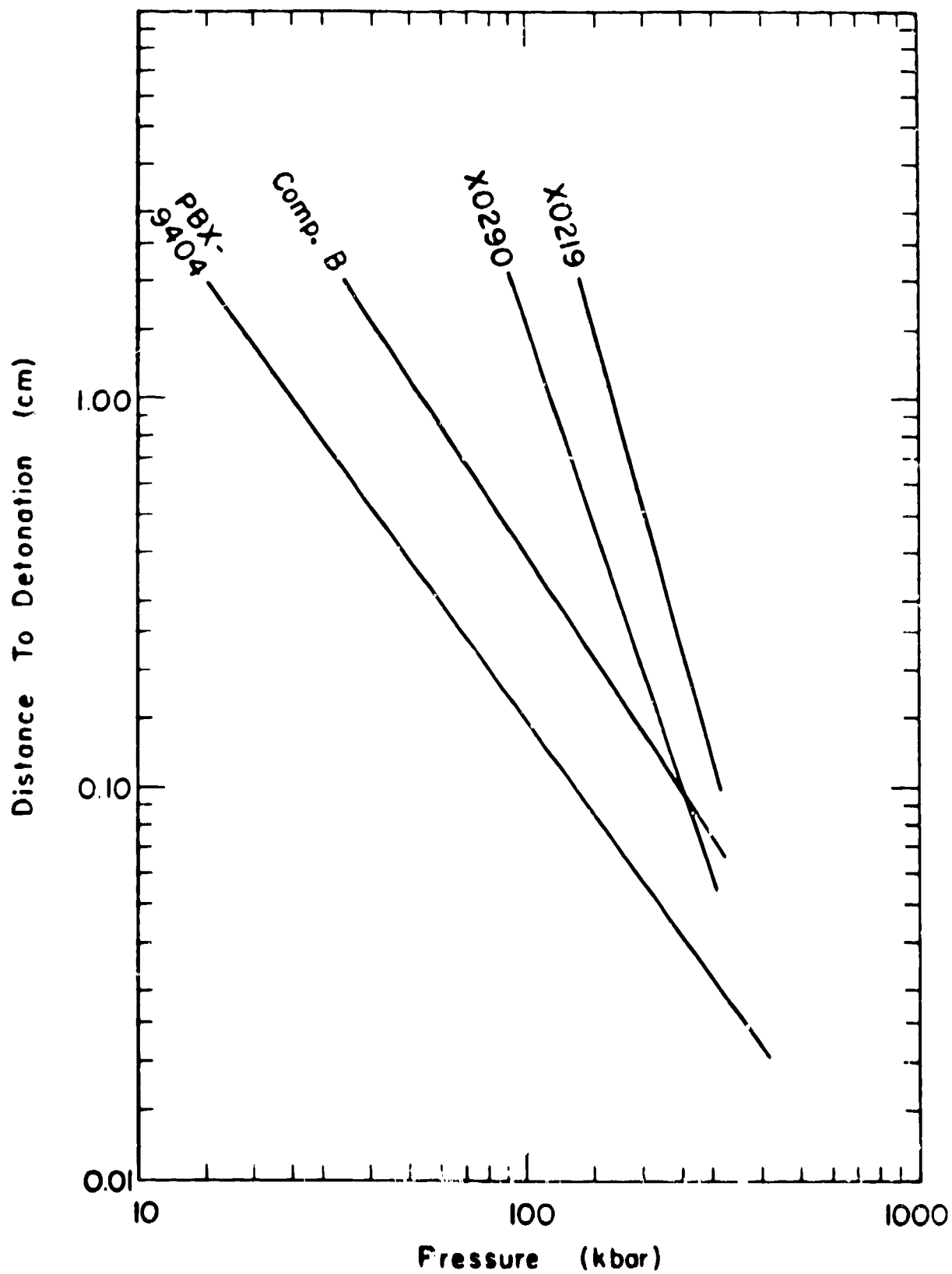


Fig. 1.
The distance of run to detonation as a function of the shock pressure.

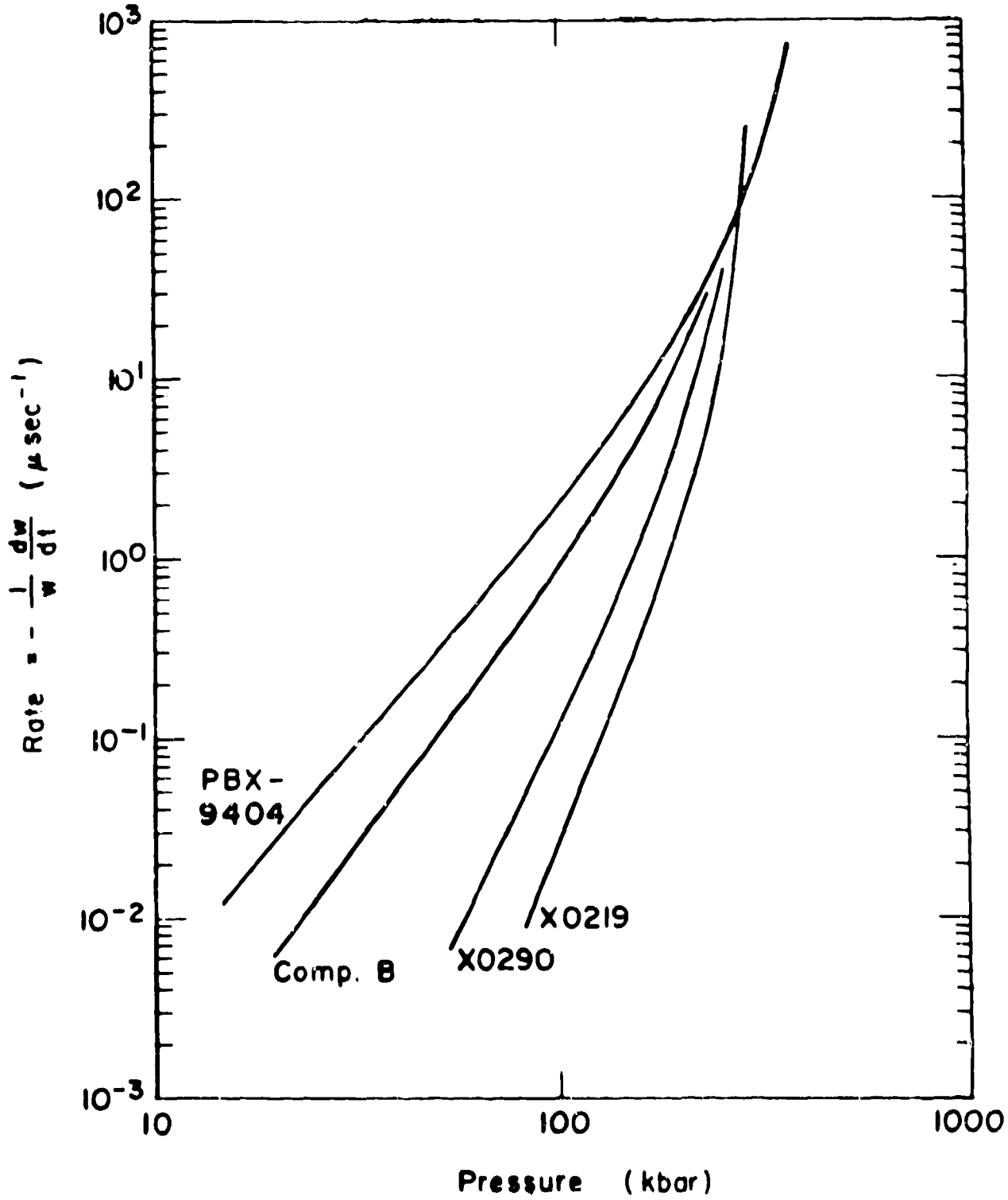


Fig. 2
 The Forest Fire decomposition rates as a function of shock pressure.

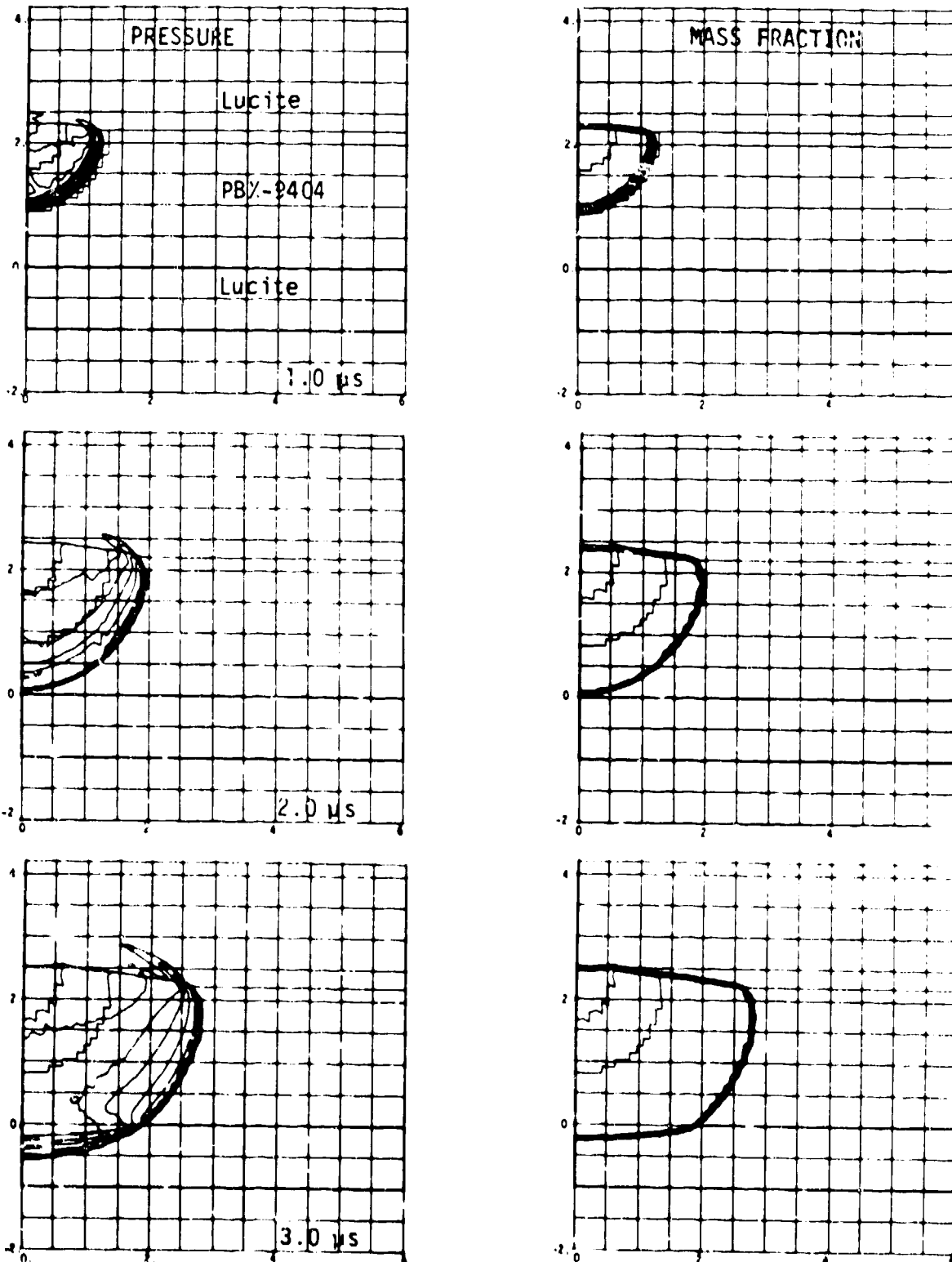


Fig. 3.

The pressure and mass fraction contours at various times for a hemispherical initiator of 6.35-mm-radius PBX-9407 surrounded by 6.35 mm of PBX-9404 initiating PBX-9404. The pressure contour interval is 50 kbar and the mass fraction contour is 0.1.

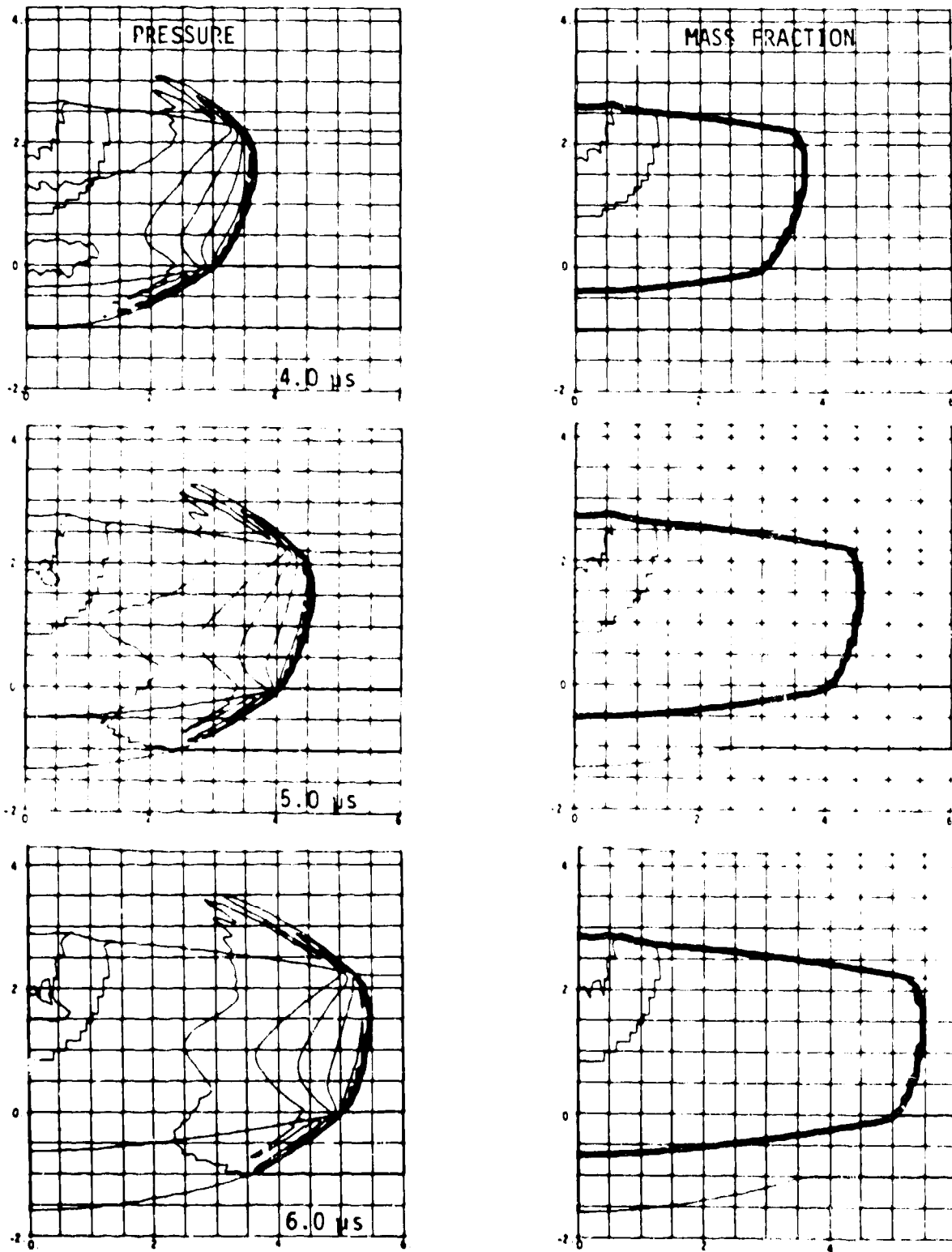


Fig. 3. (cont)

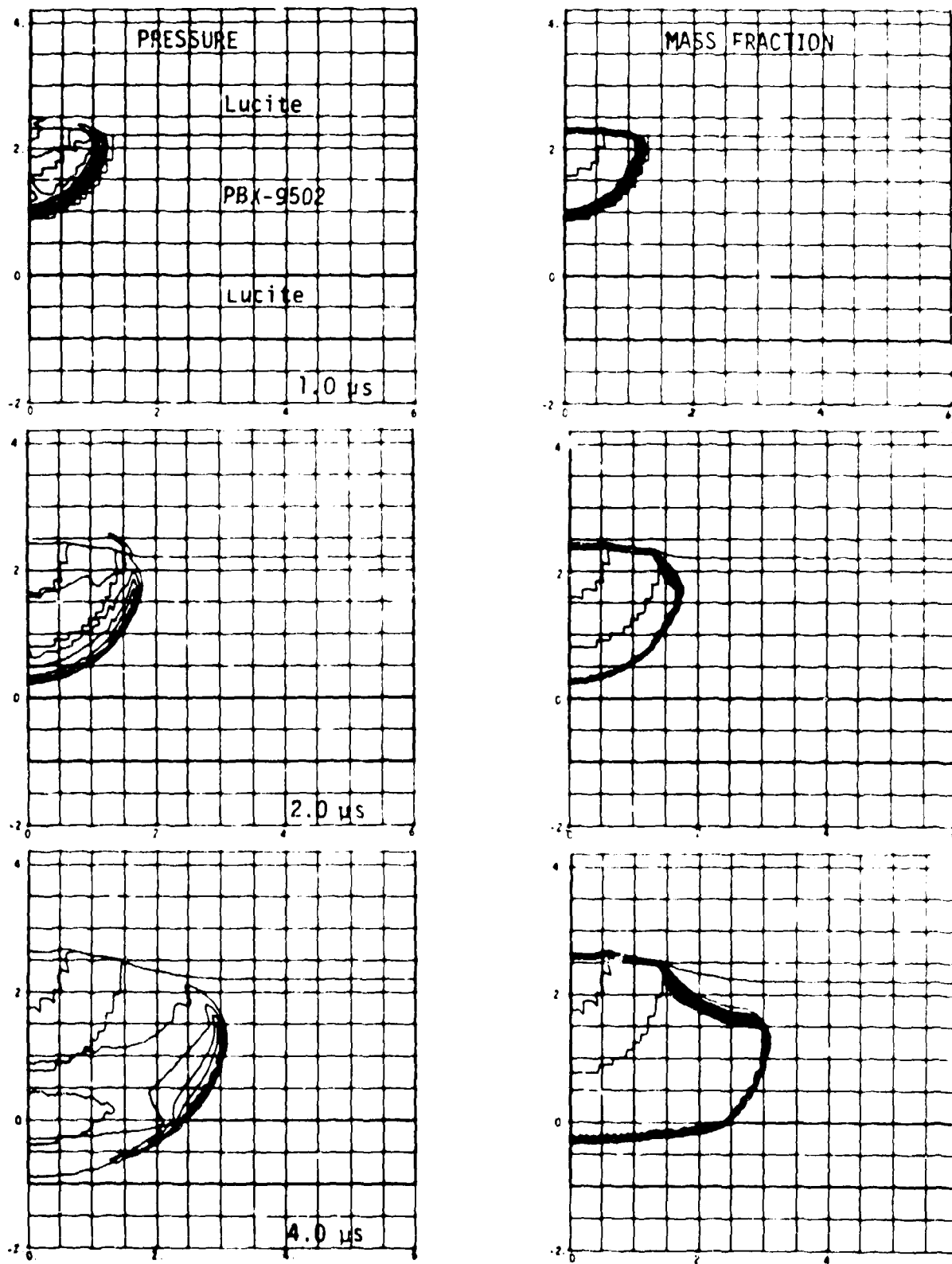


Fig. 4.

The pressure and mass fraction contours at various times for a hemispherical initiator of 6.35-mm-radius PBX-9407 surrounded by 6.35 mm of PBX-9406. Initiating PBX-9502 (X0290). The pressure contour interval is 50 kbar and the mass fraction contour is 0.1.

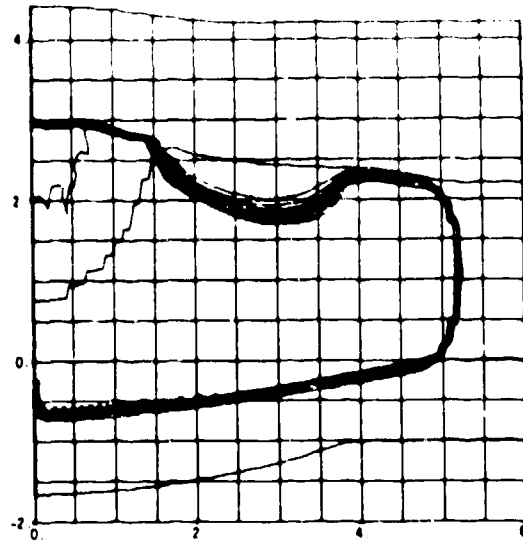
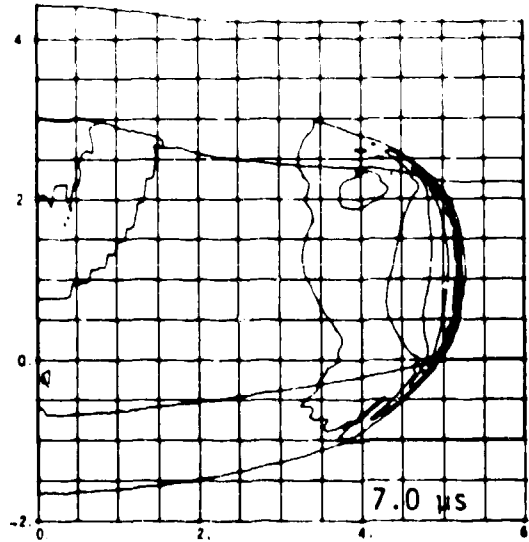
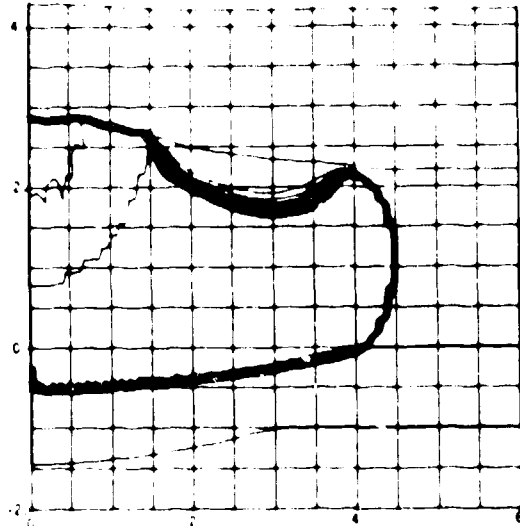
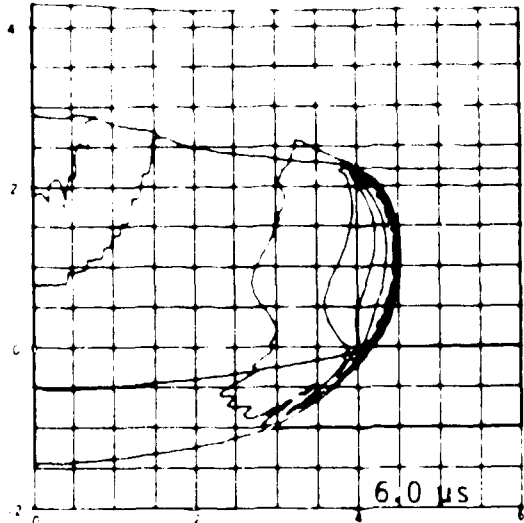
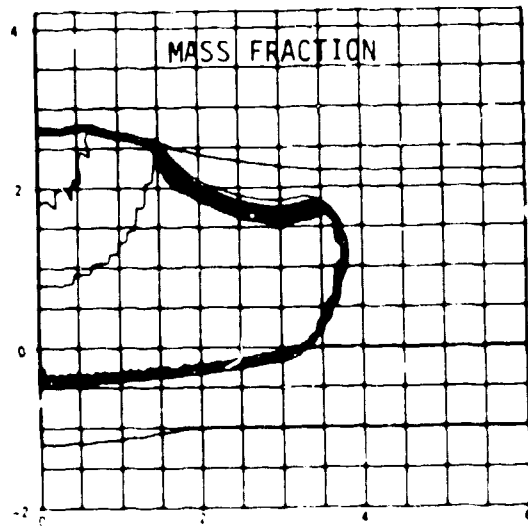
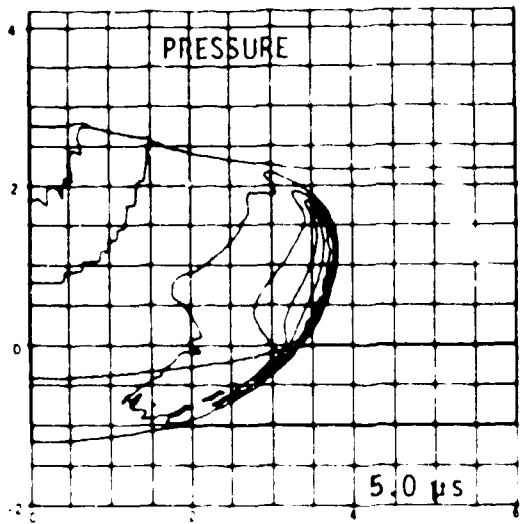


Fig. 4. (cont)

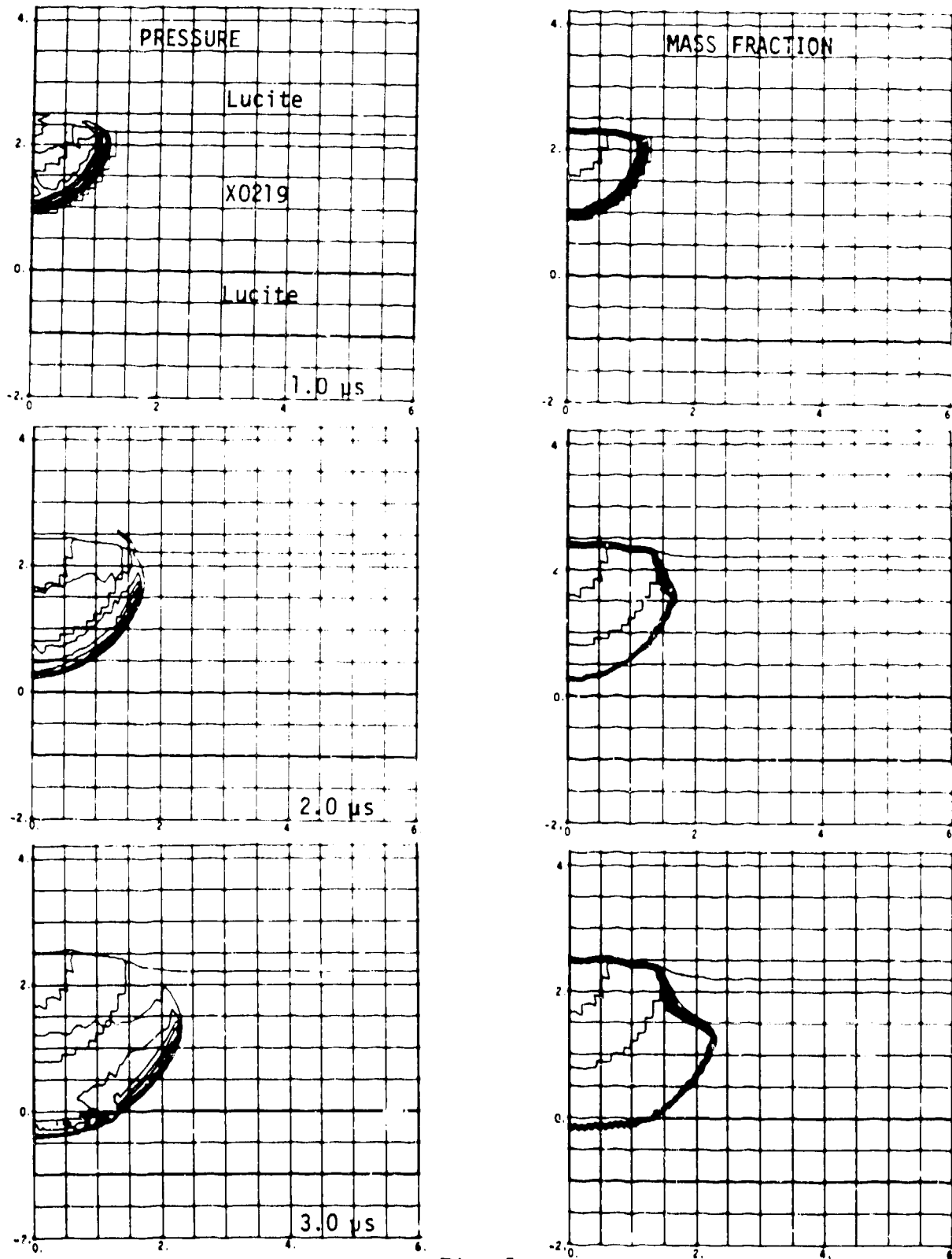


Fig. 5.

The pressure and mass fraction contours at various times for a hemispherical initiator of 6.35-mm-radius PBX-9407 surrounded by 6.35 mm of PBX-9404 initiating X0219. The pressure contour interval is 50 kbar and the mass fraction contour is 0.1.

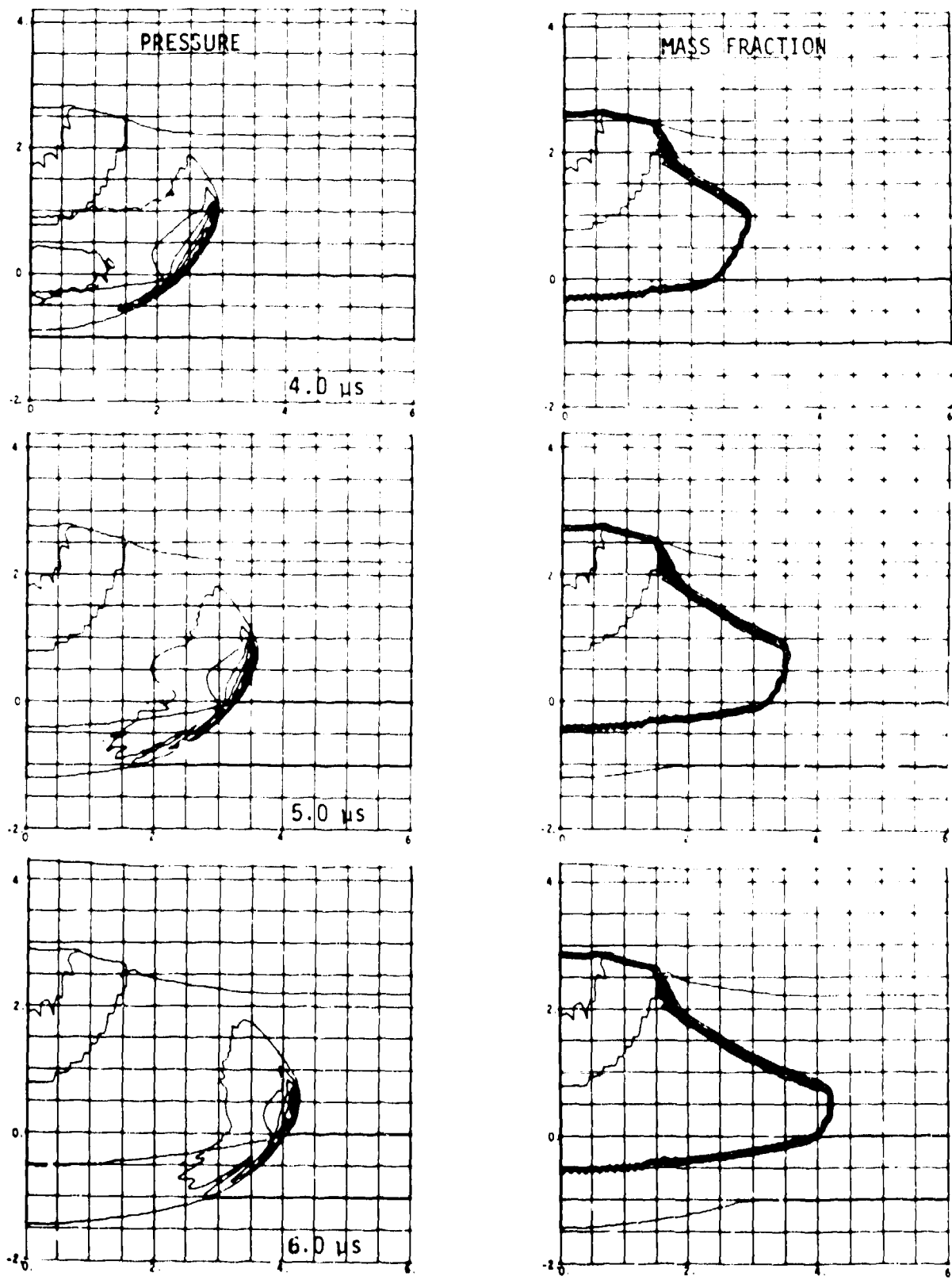


Fig. 5. (cont)

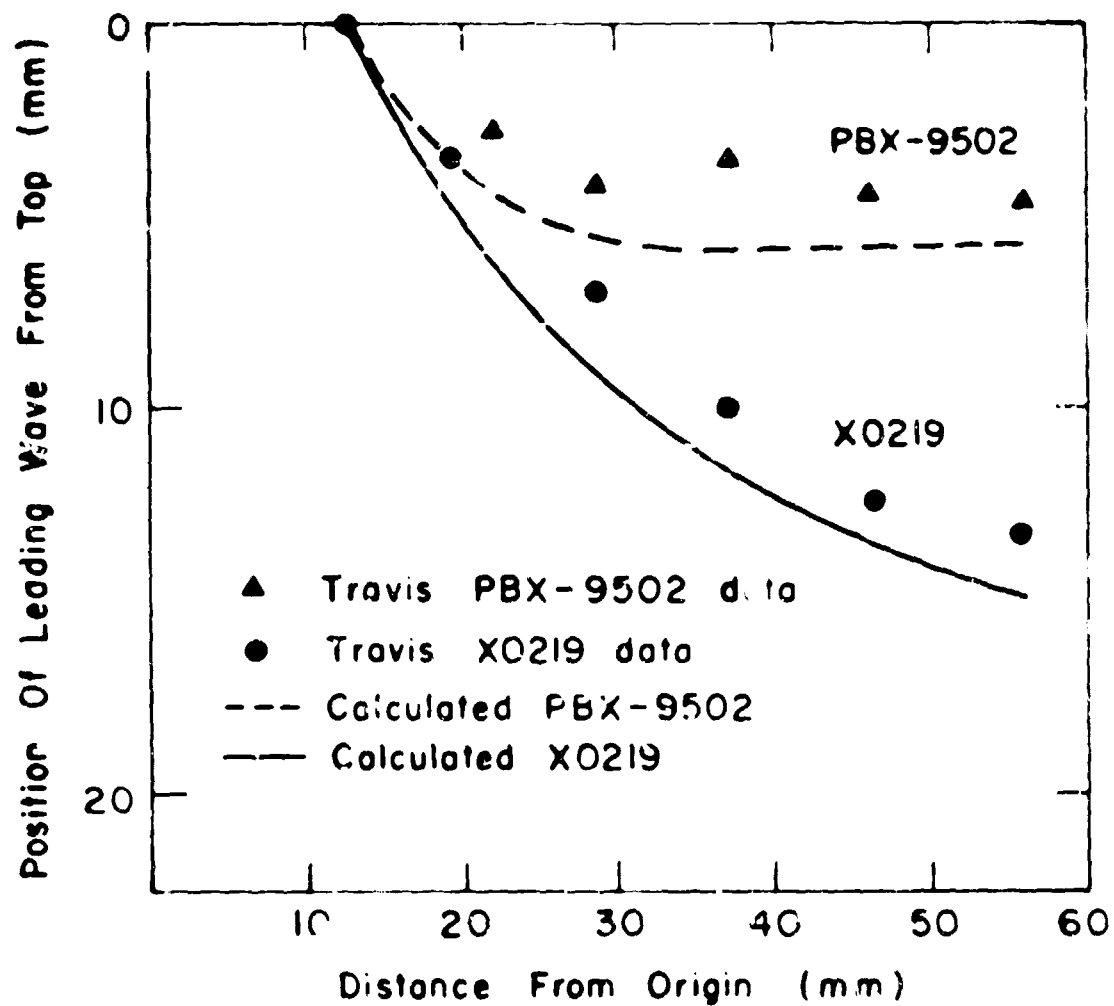


Fig. 6.
 The experimental and calculated position of the leading wave from the top of the explosive block as a function of the distance of the leading front of the wave from the origin.

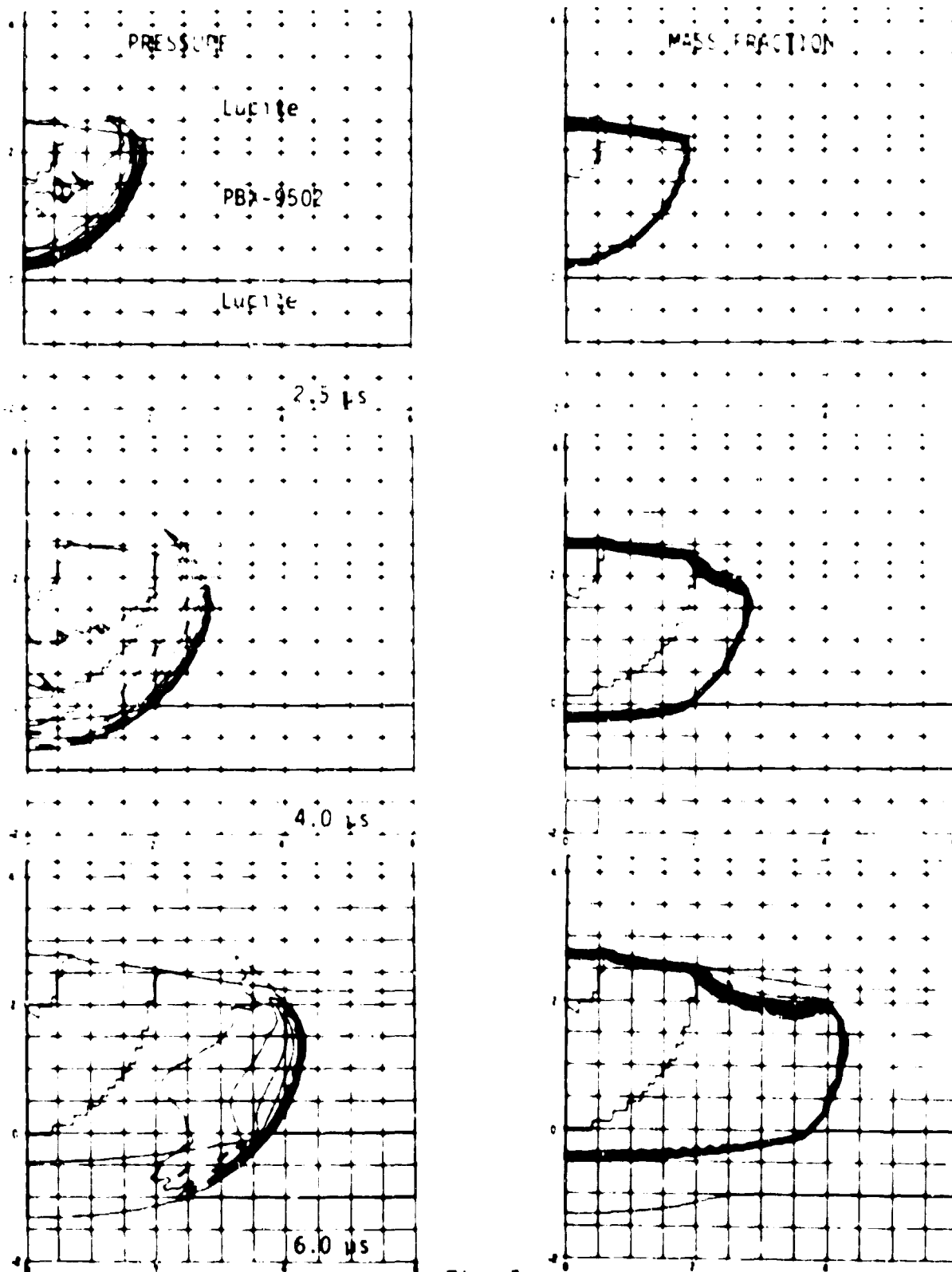


Fig. 7.

The pressure and mass fraction contours at various times for a hemispherical initiator of 6.35-mm-radius TATB at 1.7 g/cm^3 surrounded by 19.05 mm of TATB at 1.8 g/cm^3 initiating PBX-9502. The pressure contour interval is 50 kbar and the mass fraction contour is 0.1.

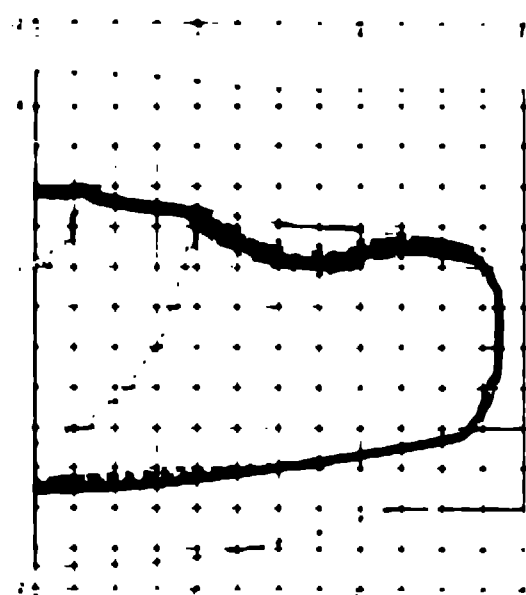
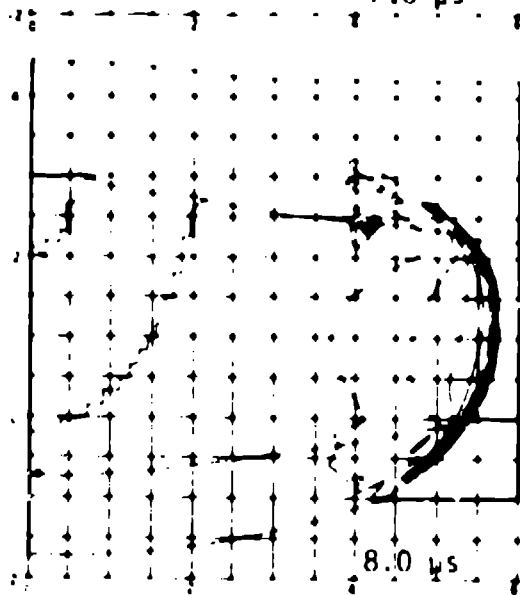
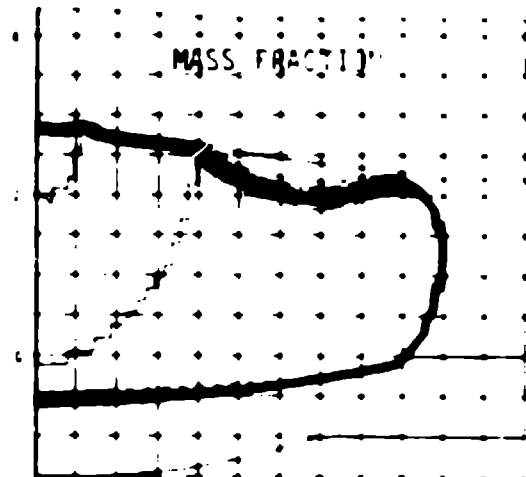
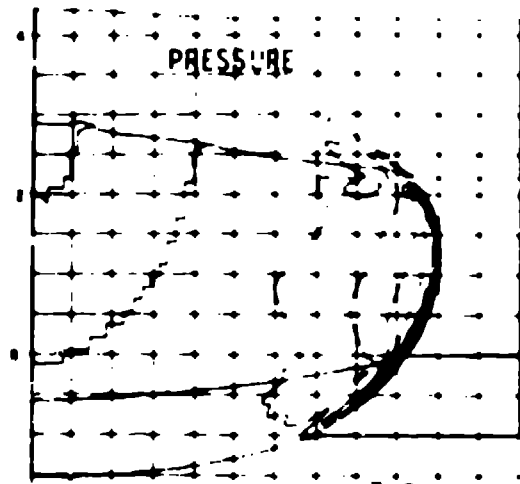


Fig. 7. (cont)

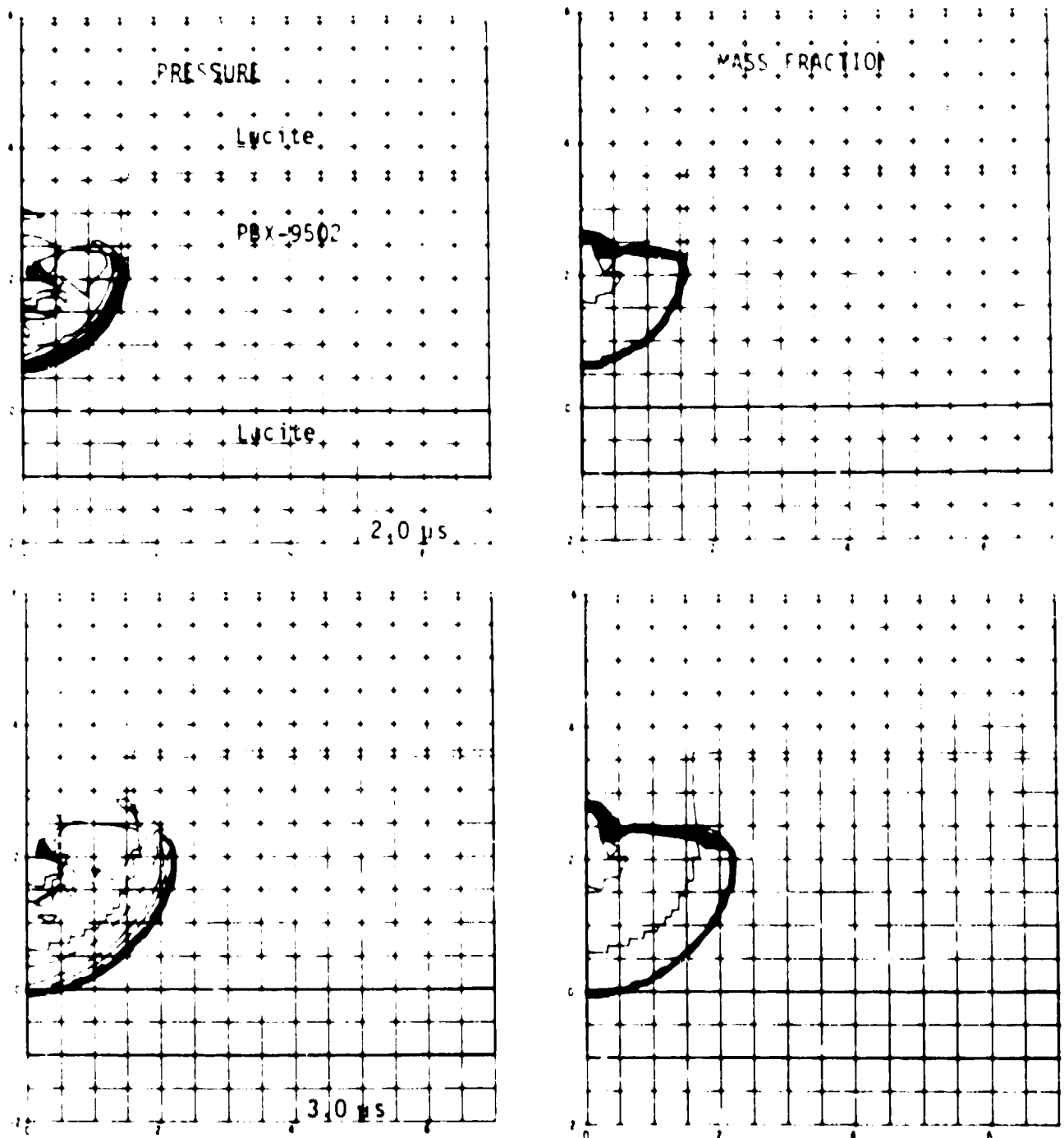


Fig. 8.
 The pressure and mass fraction contours at various times for a hemispherical initiator of 16-mm-radius X0351 initiating PBX-9502. The pressure contour interval is 50 kbar and the mass fraction contour is 0.1.

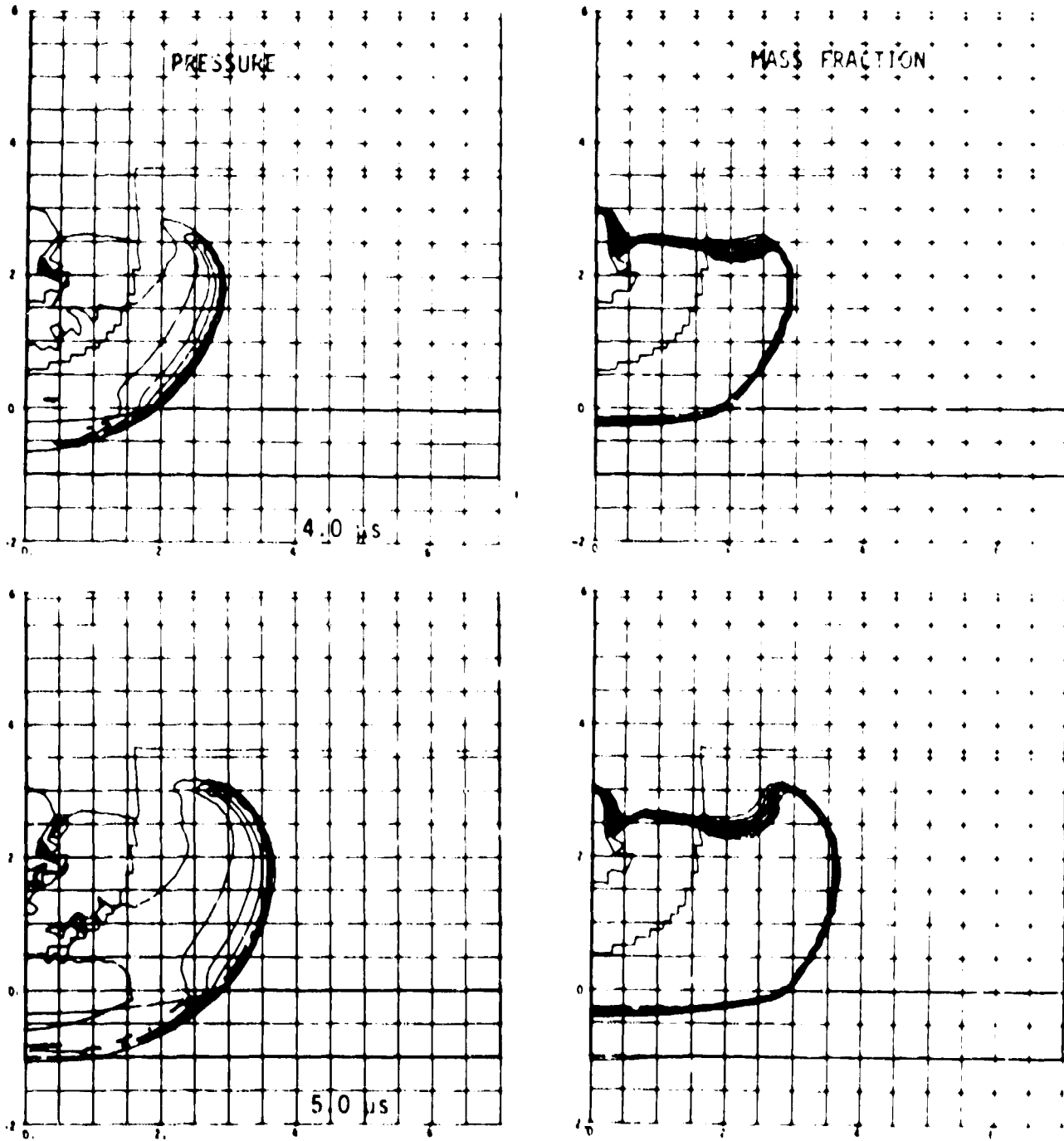


Fig. 8. (cont)

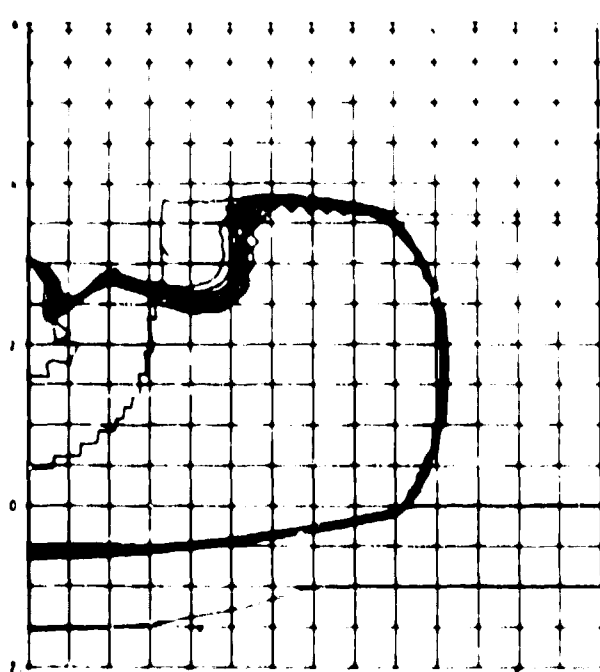
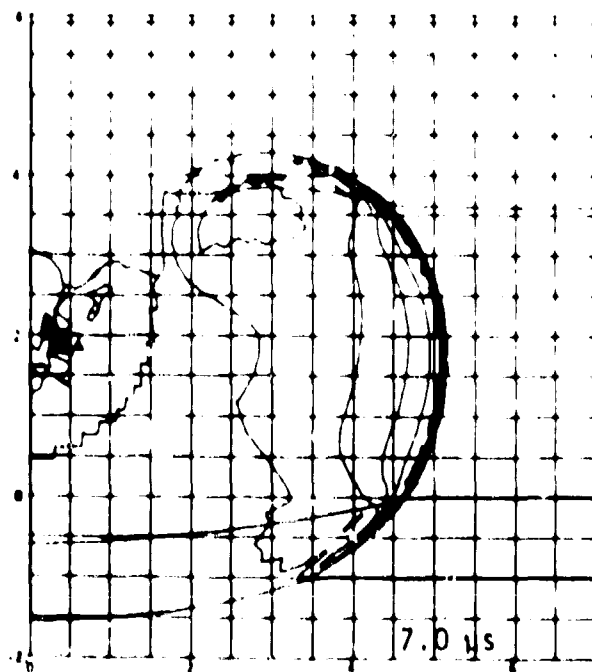
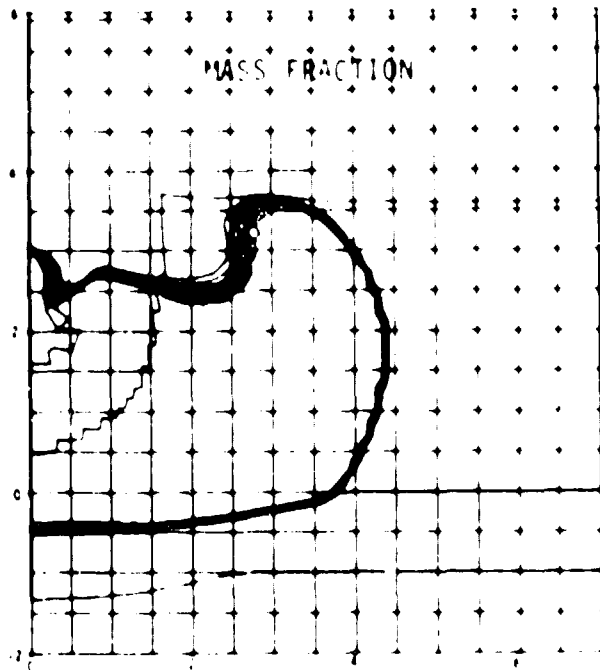
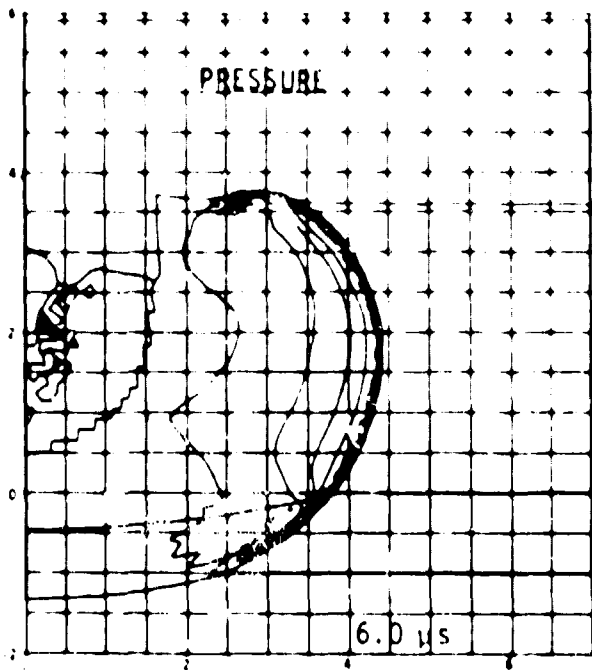


Fig. 8. (cont)

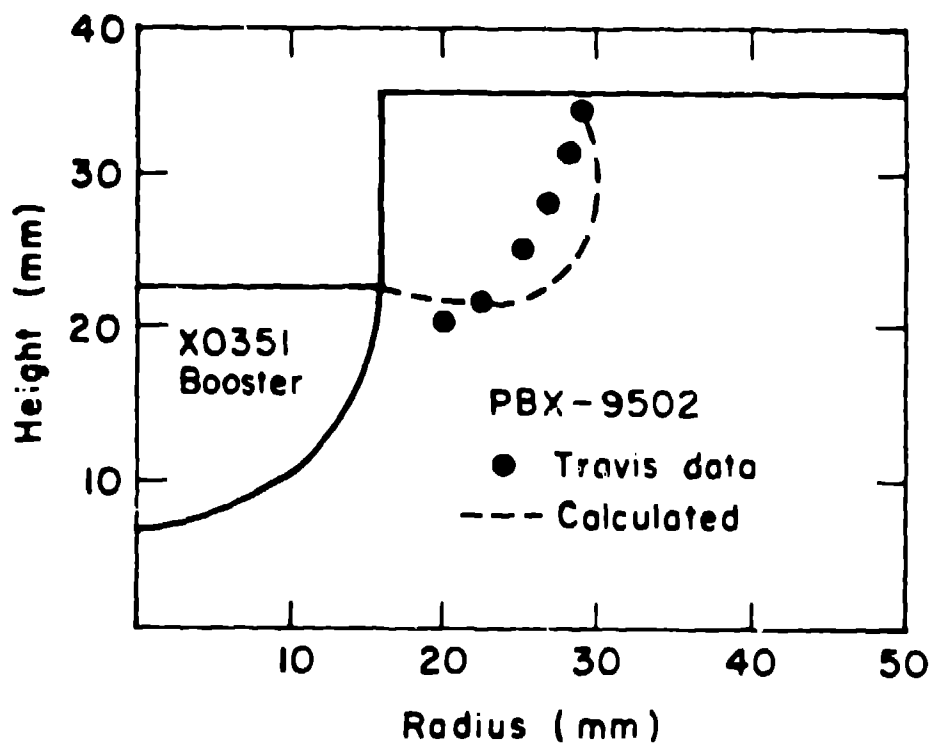


Fig. 9.
The calculated and experimental region of partially decomposed PBX-9502 when initiated by an X0351 initiator.